Environmental Earth Sciences (2021) 80:518
https://doi.org/10.1007/s12665-021-09806-0

ORIGINAL ARTICLE

Assessment of extreme climatic event model parameters estimation techniques: a case study using Tasmanian extreme rainfall

Iqbal Hossain[1] · Anirban Khastagir[2] · Most. Nazeen Aktar[2] · Monzur Alam Imteaz[1]

Received: 16 September 2020 / Accepted: 29 July 2021 / Published online: 9 August 2021
© The Author(s), under exclusive licence to Springer-Verlag GmbH Germany, part of Springer Nature 2021

Abstract

The use of generalised extreme value (GEV) distribution to model extreme climatic events and their return periods is widely popular. However, it is important to calculate the three parameters (location, scale and shape) of the GEV distribution before its application. To estimate the parameters of the GEV distribution, different parameters estimation techniques are available in literature. Nevertheless, there are no set guidelines with a view of adopting a specific parameters estimation technique for the application of the GEV distribution. The sensitivity analysis of different parameters estimation techniques, which are commonly available in the application of the GEV distribution is the main objective of this study. Extreme rainfall modelling in Tasmania, Australia was carried out using four different parameters estimation techniques of the GEV distribution. The homogeneity of the extreme data sets were tested using the Buishand Range Test. Based on the estimated errors (MSE and MAE), the L-moments parameter estimation technique is appropriate for the data series, where there is a possibility to have outliers. The GEV distribution parameters can vary considerably due to variation in the length of the data series. Finally, Fréchet (type II) GEV distribution is the most appropriate distribution for most of the rainfall stations analysed in Tasmania.

Keywords GEV distribution · Parameters estimation · Extreme rainfall · L-moments · Fréchet

Introduction

During the late 20th Century, due to augmentation of anthropogenic activities, there is a gradual surge of greenhouse gas emission (Sachindra et al. 2016). It is a common understanding that global warming and greenhouse gas emission will act as a catalyst to facilitate frequent occurrence of extreme climatic events (Crowley 2000; Sachindra et al. 2016). Intergovernmental Panel on Climate Change (IPCC) (IPCC 2012) reported that increased greenhouse gases in the atmosphere has contributed to change the patterns of rainfall. Large scale-climate drivers, initial weather conditions, regional effects and stochastic process further aggravate the processes of extreme events (Sillmann et al. 2017). Consequently, several studies (Mekanik et al. 2013; Yilmaz et al. 2014; Hossain et al. 2018a, b, 2020a) carried out analysis to identify climate change effects on rainfall using linear (multiple linear regression) and non-linear (artificial neural network, non-linear regression) models. Seasonal rainfall forecasting techniques using the influential climatic variables, e.g. ENSO, IOD were the focus of the above stated studies. Nevertheless, it was identified that linear and non-linear modelling approaches are not effectual to forecast the actual behaviour of the extreme rainfall (Hossain et al. 2020a, b). On the other hand, it is well established that the frequency and occurrence of extreme climatic events are changing globally (Fischer and Knutti 2015; Pereira et al. 2018).

Due to widespread global warming scenarios throughout the world in recent years, the changes in the extreme climatic events are evident in different parts of Australia followed by their changed frequency and occurrence. For example, Melbourne observed an incessant eleven-year drought period with cumulative rainfall continuing to be significantly below average (Khastagir and Jayasuriya 2010). Due to the continuous accumulation of carbon dioxide in the environment, the pace of climate change is aggravated (Cox et al. 2000). As a result, considerable

✉ Iqbal Hossain
ihossain@swin.edu.au

[1] Department of Civil and Construction Engineering, School of Engineering, Swinburne University of Technology, Melbourne, VIC 3122, Australia

[2] School of Engineering and Technology, RMIT University, Melbourne, VIC 3000, Australia

changes in the frequency and occurrence of extreme rainfall are expected to increase in near future (Bryson Bates 2015).

In Australian context, extreme rainfall is more common in the island state Tasmania. Although the average rainfall in some cities of Tasmania is 775 mm, the minimum rainfall could be only 31 mm per month in the summer months. Increased flood risk associated with extreme rainfall event is causing substantial losses in properties and human lives in different parts of Tasmania. Therefore, it is intrinsic to accurately predict the frequency and magnitude of extreme rainfall to prepare our future society.

The climatic system in the earth is made up of regions where the response to energy balance is different. The dynamics of each region are controlled by the local physical–chemical boundary conditions. Therefore, regional physical–chemical-biological process dictate the intrinsic patterns of climatic variability (Loubere 2012). Consequently, several climatic modes have significant influence on the variability of extreme climatic events, e.g., extreme rainfall. Nevertheless, the uneven distribution of worldwide rainfall has already been observed in many parts of the world. For example, Kumar et al. (2020) noted that there will be significant variation in the distribution of projected extreme rainfall in Bihar, India. As a result, the productivity of crops in the arid and semi-arid regions have declined inferring increased uncertainty. Ghorbani et al. (2021) observed declining rainfall trend in the central part and increasing rainfall trend in northern and southern part of Algeria. Lai and Dzombak (2019) observed significantly different extreme rainfall in the US cities. They further noted investigated that cities within the same climatic region has the potential to encounter substantially different extreme rainfall. Therefore, the importance of regional analysis is underlined by many research studies around the world in extreme climatic event study.

Extreme rainfall is generally analysed to determine flood magnitude of specified return periods for the scarce record of gauged streamflow data regions (Cannon and Innocenti 2019). Although, it is intricate to predict the historical increase in extreme rainfall due to natural variability, uncertainties in the measurement and long-term records, the observation from the large regions and climatic model's simulation are consistent with thermodynamically driven increased extreme rainfall in near future (Min et al. 2011; Westra et al. 2012; Pfahl et al. 2017). Therefore, study on the extreme rainfall analysis and forecasting is a matter of great concern throughout the world (Ávila et al. 2019). For the prediction of flood values from extreme rainfall, extreme value statistics are generally interest to the hydrologists and water resources engineers (Towler et al. 2010). The extreme value statistics projects the occurrence of future extreme rainfall through frequency analysis of the previous data (El Adlouni et al. 2007).

Frequency analysis is carried out for a series of previous observations to fit statistical probability distributions (Khaliq and Ouarda 2007). As for example, Log Pearson Type III (LPIII) distribution is recommended as a suitable general distribution for extreme value analysis as detailed in flood (McMahon and Srikanthan 1981) and fire (Khastagir 2018) frequency analyses in Australia. Although, several probability distribution functions can be used for the frequency analysis of extreme rainfall, the generalised extreme value (GEV) distribution is commonly used in extreme rainfall analysis. The GEV is statistical distribution of three parameters (location, scale, and shape). Although different methods of the GEV parameters estimation techniques are available in literature, no specific guideline was found to adopt suitable technique. However, selection of parameters estimation technique can significantly influence the return levels estimation of extreme rainfall (Lazoglou et al. 2019; Hossain et al. 2021a; Khastagir et al. 2021).

In this study, evaluation of different parameters estimation techniques of the GEV distribution was performed. Frequency analysis of Tasmanian extreme rainfall (monthly maximum from daily rainfall) were used to estimate the parameters of the GEV distribution. As higher number of GEV models that may arise from non-stationary consideration has the potential to decrease the performance of GEV selection criteria (Xavier et al. 2019), the analysis of this paper was performed considering that the rainfall pattern is stationary. The main objective of this study was to identify the most appropriate parameter estimation technique for GEV statistics. The results obtained from this study will significantly contribute to identify the most appropriate parameter estimation technique of the GEV distribution, which is commonly used for extreme rainfall analysis.

Data collection and study area

Tasmania is the island state of Australia, which is located around 240 km south from the mainland state Victoria. Average elevation of the state 104 m above the mean sea level. The climate of the state varies greatly comparing with the other parts of Australia. There is rainfall in all season in Tasmania with mild to warm summer and mild winter because of southerly marine air masses. The annual rainfall around the state is highly variable ranges from 510 to 2500 mm. There is also remarkable variation in the summer rainfall from year to year.

Wide geographic and terrestrial variation in biodiversity make Tasmania a unique heritage region in the world. However, the climate change trends of the state are coherent with the worldwide trend leading to extreme climatic events (such as extreme rainfall, drought, bushfire) (DPI 2010). Like other parts of the world, several large-scale climatic modes are significantly affecting the Tasmanian extreme rainfall (Hill et al. 2009). Therefore, study on Tasmanian extreme rainfall has the potential to reflect the global context.

From 1996 to 2009, much of the south Australian region including Tasmania experienced a persistent dry period. The long-term average rainfall declined significantly with more severity in the densely populated area, especially in all the southern cropping zone of Australia. However, significant amount of rainwater is required to maintain balance growth of Australian crops (Hossain et al. 2021b). The periodic dry episode is considered as the millennium drought in Australia.

In this study, daily rainfall data from selected 20 rainfall stations spearing all around Tasmania were collected and analysed. Figure 1 delineates the locations of the rainguage stations considered in this study. The daily rainfall data for the selected 20 rainfall stations from 1965 to 2018 was collected using SILO database, which is the Queensland Government database. Missing data filling was carried out using the data from Bureau of Meteorology (BoM) and incorporated in the SILO database.

Detailed information of the rainfall stations is shown in Table 1. The selection of rainguage stations is based on the following criteria:

- Adequate distribution of stations across Tasmania to represent all climatic conditions.
- Availability of rainfall data at a station.
- Number of years of data available.

Methodology

As mentioned earlier, historical daily rainfall data from SILO database were analysed using the extreme value theory. Monthly maximum rainfall was extracted from the collected daily data. As the removal of outliers have the potential to change the variance and the analysis may produce biased result, it is important to note that outliers of the rainfall data were not removed in this analysis.

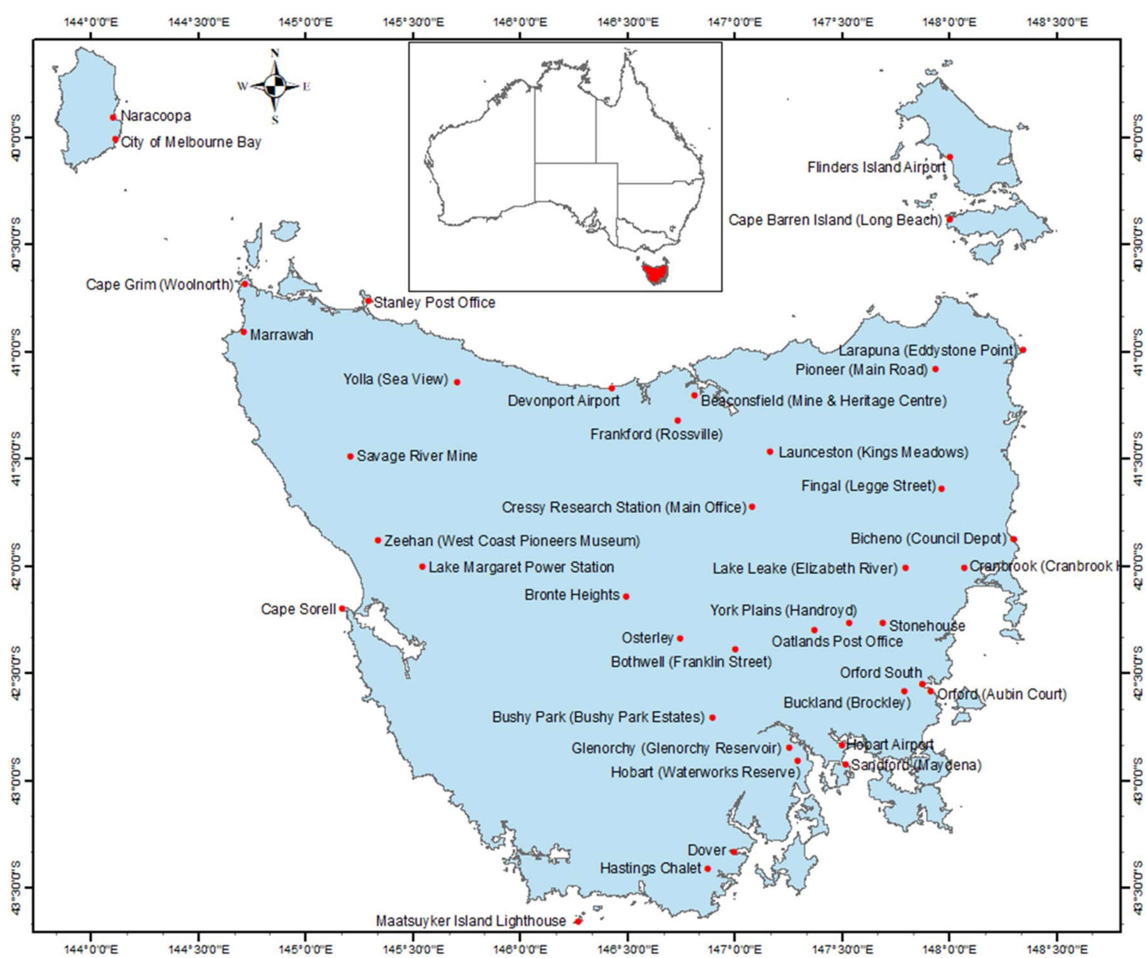

Fig. 1 Location of rainguage stations considered in this study

Table 1 Details of the meteorological stations used to estimation the GEV parameters

Station number	Station name	Latitude	Longitude	Elevation
91011	Cape Grim (Woolnorth)	– 40.6842	144.7181	15
91022	Cressy Research Station (Main Office)	– 41.7219	147.0811	148
91072	Launceston (Kings Meadows)	– 41.4664	147.1644	67
91126	Devonport Airport	– 41.1701	146.4289	8
91223	Marrawah	– 40.9089	144.7094	107
92006	Buckland (Brockley)	– 42.5847	147.7908	58
92008	Cranbrook (Cranbrook House)	– 42.0117	148.0747	17
92012	Fingal (Legge Street)	– 41.6428	147.9664	237
92030	Pioneer (Main Road)	– 41.0825	147.9353	120
92047	Stonehouse	– 42.2683	147.6936	375
94008	Hobart Airport	– 42.8339	147.5033	4
94020	Dover	– 43.333	146.998	20
94030	Hobart Botanical Gardens	– 42.8667	147.3322	27
95003	Bushy Park (Bushy Park Estates)	– 42.7097	146.8983	27
96002	Bronte Heights	– 42.1423	146.4932	710
97000	Cape Sorell	– 42.1986	145.17	19
97047	Savage River Mine	– 41.4892	145.2083	352
97054	Zeehan (West Coast Pioneers Museum)	– 41.8822	145.3358	175
98004	Naracoopa	– 39.9078	144.0998	20
99005	Flinders Island Airport	– 40.0911	148.0024	9

However, assessment of the variation in the extreme data sets, homogeneity was performed using the Buishand's range test. The adjusted partial sum in the Buishand range test can be represented according to Eq. 1 (Buishand 1982).

$$S_k^* = \sum_{i=1}^{n} \left(Y_i - \overline{Y} \right) \tag{1}$$

where Y_i is the extremely rainfall for the ith time step, $\overline{Y}$ is the average of extreme rainfall data series and is the number of observations. The re-scaled adjusted range (R) factor is then measured to estimate $R/\sqrt{n}$ to compare with critical values Of Buishand (Buishand 1982). The magnitude of R is estimated from the difference between the maximum and minimum value of S_k^*.

Asymptotic extreme value models are generally fitted to identify the extremal behaviour of the climatic events especially for short series of data. It was evidenced from the observations that the daily extreme rainfall follows extreme value distribution with heavy upper tail (Papalexiou and Koutsoyiannis 2013). Therefore, three parameters GEV distribution has been widely applied to describe the characteristics of extreme climatic events, e.g. rainfall, floods, wind speed, snow depth, wave heights and other maxima. The mathematical application of the GEV distribution is also very attractive in extreme events characterisation (Hosking 1990).

Extreme value distribution

In this study, the GEV distribution was used for the frequency analysis of Tasmanian extreme rainfall. The GEV distribution is suggested for the extreme data generated using the block-maxima approach (Park et al. 2011). Since our extreme rainfall data were generated using block-maxima approach (monthly maximum from daily record), the GEV distribution was used in this study. The cumulative distribution function of the GEV distribution can be found in most of the recently conducted extreme data analysis research. The function has been re-written here according to Eq. 2:

$$G(Y;\theta) = exp\left\{ -\left[1 + \xi \left(\frac{Y-\mu}{\sigma} \right) \right]^{-1/\xi} \right\} \tag{2}$$

where Y represents the extreme rainfall data (in this case monthly maximum daily rainfall) and $\theta(\mu, \sigma, \xi)$ represents the parameters of the GEV distribution.

The physical origin of the extreme events suggests that their distribution follow in any of the three extreme value types (types I, II and III) (Martins and Stedinger 2000). The GEV distribution has three types of parameters: location (μ), scale (σ) and shape (ξ). Depending on the values of the parameters, the distribution can follow either Gumbel, or Fréchet or Weibull type GEV (Park et al. 2011). For the shape parameter $\xi = 0$, the distribution becomes Gumbel (type I) class of normal, log-normal, gamma or exponential distribution. The positive shape parameter ($\xi > 0$) produces Fréchet (type II) distribution and negative shape parameter ($\xi < 0$) produce Weibull (type III) distribution.

Parameters estimation

The common problem in the application of statistical distribution is the estimation of the unknown parameters (Hosking 1990). The support of the GEV distribution shown in Eq. 1 depends on the appropriate estimation of its parameters. There are different techniques available to estimate of the parameters of the GEV distribution. Stationary vs non-stationary rainfall is still debatable. For example, Yilmaz et al. (2014), Yilmaz and Perera (2014) could not detect the presence of non-stationarity in the extreme rainfall analysis in Melbourne. Therefore, this study was performed considering the stationary behaviour of extreme rainfall data. However, the parameters of the GEV statistics can be modified to incorporate the non-stationarity of rainfall data (Coles 2001; Towler et al. 2010). In this research, the parameters of the GEV distribution were estimated using four different methods: MLE, GMLE, Bayesian and L-moments.

The maximum likelihood estimation (MLE) method

The maximum likelihood estimation (MLE) is a powerful approach to estimate the parameters of the GEV distribution where data length are relatively short (Coles and Dixon 1999). Therefore, the method has been used in several studies (Towler et al. 2010) in estimating the parameters of the non-stationary GEV models. The values of the parameters (μ, σ, ξ) that maximises the likelihood function are the estimated parameters. In practice, the MLE is expressed as the log likelihood (L) function of the GEV distribution as shown in Eq. 3.

$$L(\theta;y_i) = \sum_{i=1}^{N} log\{G(\theta;y_i)\} \tag{3}$$

The log likelihood function of the Eq. 2 can be expanded according to Eq. 4 as follows (Yoon et al. 2010).

$$log[L(\theta;y_i)] = -N \times log(\sigma) - \left(1 + \frac{1}{\xi}\right) \sum_{i=1}^{N} log(x_i) - \sum_{i=1}^{N} (x_i)^{-1/\xi} \tag{4}$$

where $\theta = (\mu, \sigma, \xi)$ and $x_i = \left[1 + \xi\left(\frac{y_i - \mu}{\sigma}\right)\right]$.

The partial derivatives of the log-likelihood functions can be solved to estimate the parameters of the GEV distribution. The negative log likelihood function also can be minimised to find out the parameters using MLE method (Katz 2013). The negative log likelihood functions are minimised with respect to three parameters: location, scale, and shape parameters. However, the method is computationally intensive (Nakajima et al. 2012). Moreover, the method underestimates the negative value of the shape parameter for small or moderate sample size (Park 2005).

The generalised maximum likelihood estimation (GMLE) method

To overcome the limitation of the MLE method for small or moderate sample size, the generalised maximum likelihood (GMLE) method was developed (Park 2005). The method has been developed based on the MLE method. The method included an additional constraint of the shape parameters to eliminate the invalid results that may be produced in MLE method. The method uses a prior distribution of the shape parameter to avoid the value of the parameters being large negative (Park 2005; Yoon et al. 2010).

$$GL(y_i;\mu, \sigma, \xi) = L(y_i;\mu, \sigma, \xi)\pi(\xi) \tag{5}$$

Consequently, the generalised log-likelihood of Eq. 4 can be expanded as Eq. 6.

$$\begin{aligned} log[L(\theta;y_i)] = &-N \times log(\sigma) - \left(1 + \frac{1}{\xi}\right) \sum_{i=1}^{N} log(x_i) \\ &- \sum_{i=1}^{N} (x_i)^{-1/\xi} + +ln\{\pi(\xi)\} \end{aligned} \tag{6}$$

To maximize this function for the estimation of the GEV parameters, Newton Raphson can be used (Yoon et al. 2010).

The Bayesian method

Like the GMLE method, the Bayesian method was also developed to overcome the limitation of small sample size of the extreme time-series data. The fundamental of Bayesian method require the prior distribution of the GEV parameters $\theta = (\mu, \sigma, \xi)$. Therefore, the essential of Bayesian method is a prior distribution $f(\theta)$ and a likelihood $f(Y\text{I}\theta)$ (Coles and Tawn 2005). Bayes theorem balances these two sources produces the posterior distribution $f(\theta\text{I}Y)$, such that:

$$f(\theta\text{I}Y)\alpha f(\theta)f(Y\text{I}\theta) \tag{7}$$

where Y is the historical data set and $\theta = (\mu, \sigma, \xi)$ is the location, scale and shape parameter of the GEV distribution.

The posterior probability density of the GEV parameters $p(\theta\text{I}Y)$ can be obtained by the well-known Bayes theorem as follows:

$$p(\theta \mathrm{I} Y) = \frac{f(Y\mathrm{I}\theta)\pi(\theta)}{\int f(Y\mathrm{I}\theta)\pi(\theta)d\theta} \tag{8}$$

where $p(\theta \mathrm{I} Y)$ is the posterior probability density of the GEV parameters, Y is the observations, $f(Y\mathrm{I}\theta)$ is the likelihood of the observations and $\pi(\theta)$ is prior probability density of the GEV parameters.

Since analytical determination of the posterior distribution is difficult, Markov Chain Monte Carlo algorithm can be used to derive the parameters $\pi(\theta)$. Details of the method can be found in Gilks et al. (1995).

L-moments method

The L-moments is based on the probability weighted moments which describe the shape of probability distributions. The method can be defined as the linear combination of probability weighted moments (Hosking 1990). The method estimates the parameters of the statistical distribution by equating the first p-sample L-moments to the corresponding population sample. The L-moment method is less affected from data variability and outliers. Moreover, the method is comparatively unbiased for the small number of samples. Details of the L-moment method can be found in Hosking (1990).

The GEV distribution parameters according to the L-moments method can be described as follows (Hosking and Wallis 1993; Huard et al. 2010).

$$\mu = l_1 + \frac{\sigma[\Gamma(1+\xi) - 1]}{k} \tag{9}$$

$$\sigma = \frac{\xi l_2}{\Gamma(1+\xi)\left(1 - 2^{-\xi}\right)} \tag{10}$$

$$\xi = 7.8590z + 2.9554z^2 \tag{11}$$

where μ, σ and ξ are the location, scale and shape parameters respectively; l_1, l_2 and l_3 are the L-moments and

$$z = \frac{2l_2}{l_3 + 3l_2} - \frac{ln(2)}{ln(3)} \tag{12}$$

Results and discussions

This section presents the outcomes of analysis performed in this research, including subsequent discussions. The application of homogeneity test, three parameters (location, scale and shape) of the GEV technique were obtained using the computer programming language R and RStudio.

Table 2 Buishand range homogeneity test result for the selected rainfall station in Tasmania from 1965 to 2018

Station number	Station name	Skewness	Coefficient of variation	Test Statistics	*p* value
91011	Cape Grim (Woolnorth)	1.98	0.62	1.421	0.203
91022	Cressy Research Station (Main Office)	2.29	0.67	0.912	0.874
91072	Launceston (Kings Meadows)	1.46	0.60	1.394	0.228
91126	Devonport Airport	1.68	0.65	1.218	0.442
91223	Marrawah	2.16	0.60	1.393	0.242
92006	Buckland (Brockley)	2.49	0.98	1.205	0.459
92008	Cranbrook (Cranbrook House)	2.37	0.99	0.970	0.804
92012	Fingal (Legge Street)	2.28	0.90	1.124	0.583
92030	Pioneer (Main Road)	2.10	0.69	0.884	0.903
92047	Stonehouse	1.76	0.82	1.232	0.422
94008	Hobart Airport	1.66	0.77	1.508	0.141
94020	Dover	2.26	0.69	1.152	0.541
94030	Hobart Botanical Gardens	2.31	0.82	1.573	0.096
95003	Bushy Park (Bushy Park Estates)	1.40	0.61	2.102	0.003
96002	Bronte Heights	1.47	0.53	1.107	0.609
97000	Cape Sorell	1.45	0.48	2.227	0.001
97047	Savage River Mine	1.29	0.43	1.304	0.330
97054	Zeehan (West Coast Pioneers Museum)	1.48	0.43	1.558	0.107
98004	Naracoopa	1.83	0.61	1.224	0.434
99005	Flinders Island Airport	2.17	0.76	1.266	0.375

The extent of the variability amongst the time-series extreme rainfall were determined using the statistical tests skewness and coefficient of variation. Estimated values of the skewness and coefficient of variance are shown in Table 2. From Table 2, it was observed that estimated values of the skewness were positive for all the rainfall stations implying that the right tail of the distribution is longer. It was also detected that estimated coefficient of variance was less than one for all the selected meteorological stations indicating that the variation of monthly maximum rainfall is considerably low.

Homogeneity of time series observations reflects the variability of data sets. Location, instruments or recording time may cause non-homogeneity of observed data sets (Wijngaard et al. 2003). Nevertheless, assumption of homogeneity is essential for the statistical hypothesis testing on meteorological observation. In this research, Buishand Range homogeneity test was performed to identify whether the time series is homogeneous. The test was applied for 5% significant level. The outcomes of the homogeneity analysis for the selected 20 rainfall stations are shown in Table 2. The critical value of the test statistics was determined as 1.75 from Buishand (1982). The result of the Buishand Range homogeneity test indicated that the test statistic is lower than the critical value for all the rainfall stations except two as shown in Table 2. The possible reason for the non-homogeneity of two stations may be due to the changes in the surrounding environment or instrumentation inaccuracy or changes in the calculation procedure for the missing value (Wijngaard et al. 2003; Domonkos 2015). Since extreme rainfall data for 90% of the selected meteorological stations are homogeneous, statistical hypothesis can be applied with confidence.

After determining the homogeneity of the extreme rainfall data, the GEV distribution was fitted using the four different parameters estimation techniques. The parameters of the GEV distribution were estimated for four different time-series using four different parameters estimation techniques. Due to the page limitation, only the one time-series analysis (whole study period) has been provided in this article. The estimated GEV parameters of the analysis for the whole analysis period (1965–2018) are shown in Tables 3, 4, 5, 6 for the MLE, GMLE, Bayesian and L-moments techniques.

It has been noted that the shape parameter (ξ) of the GEV distribution is positive for all the considered rainfall stations except station 97047. The statement is true for any of the methods considered in this study as evidenced from Tables 3, 4, 5, 6 for the whole study period. This implies that the GEV is Fréchet (type II) distribution (except station #97047) for the data series from 1965 to 2018. The outcomes of Table 3 suggest that the type of the GEV distribution to be used in extreme climatic modelling did not depend on the parameter estimation technique. The observed negative shape parameter can be attributed by the influence of

Table 3 Estimated GEV parameters using MLE technique rainfall data from 1965 to 2018

Station #	Location			Scale			Shape		
	95% lower CI	Estimate	95% upper CI	95% lower CI	Estimate	95% upper CI	95% lower CI	Estimate	95% upper CI
91001	16.35	17.265	18.18	9.828	10.51	11.192	0.006	0.066	0.125
91022	11.652	12.326	13	7.334	7.835	8.335	0.028	0.081	0.134
91072	13.392	14.125	14.859	8.049	8.579	9.11	− 0.026	0.025	0.075
91126	13.732	14.549	15.366	8.776	9.389	10.001	0.023	0.082	0.14
91223	14.084	14.75	15.416	7.179	7.686	8.193	0.068	0.126	0.183
92006	9.554	10.267	10.98	7.314	7.98	8.646	0.379	0.459	0.54
92008	9.685	10.444	11.204	7.786	8.5	9.215	0.388	0.468	0.549
92012	10.141	10.859	11.578	7.524	8.144	8.765	0.266	0.338	0.409
92030	16.092	17.01	17.929	9.747	10.468	11.19	0.112	0.176	0.24
92047	10.771	11.484	12.197	7.365	7.991	8.618	0.286	0.362	0.438
94008	8.894	9.487	10.079	6.126	6.623	7.119	0.207	0.282	0.357
94020	12.738	13.38	14.022	6.899	7.409	7.918	0.145	0.206	0.266
94030	9.45	10.065	10.68	6.44	6.952	7.464	0.208	0.278	0.348
95003	9.649	10.183	10.718	5.665	6.07	6.475	0.028	0.092	0.156
96002	13.572	14.204	14.836	6.851	7.316	7.781	− 0.012	0.043	0.098
97000	16.454	17.111	17.769	7.163	7.642	8.121	− 0.018	0.035	0.088
97047	21.857	22.685	23.512	9.173	9.757	10.342	− 0.072	− 0.027	0.017
97054	27.085	28.056	29.026	10.694	11.391	12.087	− 0.038	0.01	0.058
98004	13.641	14.334	15.027	7.428	7.957	8.485	0.058	0.118	0.179
99005	11.889	12.623	13.356	7.797	8.381	8.965	0.141	0.205	0.269

Table 4 Estimated GEV parameters using GMLE technique rainfall data from 1965 to 2018

Station #	Location			Scale			Shape		
	95% lower CI	Estimate	95% upper CI	95% lower CI	Estimate	95% upper CI	95% lower CI	Estimate	95% upper CI
91011	16.158	17.07	17.982	9.763	10.437	11.111	0.04	0.104	0.168
91022	11.543	12.217	12.892	7.306	7.806	8.305	0.052	0.11	0.168
91072	13.196	13.93	14.663	8.001	8.526	9.05	0.014	0.071	0.128
91126	13.58	14.397	15.214	8.726	9.334	9.943	0.051	0.115	0.179
91223	14.008	14.673	15.338	7.163	7.669	8.175	0.087	0.148	0.209
92006	9.57	10.283	10.996	7.313	7.978	8.642	0.374	0.453	0.533
92008	9.703	10.463	11.223	7.785	8.498	9.211	0.381	0.462	0.542
92012	10.131	10.849	11.568	7.524	8.145	8.766	0.269	0.341	0.413
92030	16.012	16.929	17.847	9.727	10.448	11.17	0.127	0.194	0.26
92047	10.766	11.479	12.192	7.364	7.991	8.618	0.287	0.364	0.44
94008	8.871	9.463	10.055	6.121	6.617	7.114	0.215	0.291	0.367
94020	12.701	13.343	13.985	6.897	7.407	7.918	0.156	0.218	0.28
94030	9.428	10.043	10.657	6.437	6.949	7.462	0.215	0.286	0.357
95003	9.549	10.082	10.615	5.627	6.029	6.43	0.058	0.127	0.195
96002	13.416	14.048	14.679	6.802	7.261	7.721	0.025	0.087	0.149
97000	16.288	16.944	17.601	7.115	7.589	8.063	0.02	0.08	0.14
97047	21.999	22.823	23.646	9.173	9.757	10.341	− 0.089	− 0.05	− 0.012
97054	26.792	27.763	28.734	10.624	11.312	12.001	0.005	0.062	0.118
98004	13.548	14.241	14.933	7.402	7.929	8.455	0.08	0.144	0.207
99005	11.841	12.574	13.307	7.788	8.373	8.957	0.153	0.219	0.285

Table 5 Estimated GEV parameters using Bayesian technique rainfall data from 1965 to 2018

Station #	Location			Scale			Shape		
	95% lower CI	Estimate	95% upper CI	95% lower CI	Estimate	95% upper CI	95% lower CI	Estimate	95% upper CI
91011	16.276	17.238	18.238	9.826	10.542	11.346	0.006	0.068	0.135
91022	11.534	12.303	13.051	7.323	7.87	8.445	0.028	0.084	0.147
91072	13.496	14.231	15.218	8.079	8.636	9.232	− 0.029	0.025	0.084
91126	13.629	14.531	15.388	8.762	9.409	10.103	0.022	0.085	0.153
91223	13.948	14.695	15.435	7.133	7.694	8.307	0.067	0.129	0.193
92006	9.505	10.268	11.082	7.323	8.028	8.791	0.376	0.463	0.558
92008	9.631	10.384	11.307	7.76	8.501	9.295	0.383	0.472	0.564
92012	10.017	10.973	11.742	7.525	8.255	8.987	0.259	0.336	0.419
92030	15.966	17.012	18.115	9.711	10.522	11.379	0.112	0.18	0.256
92047	10.616	11.451	12.321	7.305	7.999	8.719	0.279	0.363	0.451
94008	8.859	9.491	10.178	6.124	6.665	7.288	0.206	0.285	0.366
94020	12.684	13.328	14.056	6.852	7.414	8.022	0.142	0.209	0.276
94030	9.382	10.071	10.764	6.417	6.985	7.569	0.206	0.28	0.358
95003	9.609	10.186	10.859	5.643	6.094	6.58	0.024	0.094	0.17
96002	13.433	14.257	15.094	6.845	7.366	7.912	− 0.014	0.045	0.112
97000	16.185	17.015	17.848	7.142	7.634	8.157	− 0.016	0.04	0.098
97047	21.91	22.691	23.549	9.181	9.79	10.479	− 0.068	− 0.024	0.024
97054	26.885	28.204	29.661	10.683	11.472	12.314	− 0.043	0.01	0.069
98004	13.483	14.254	15.421	7.343	7.972	8.651	0.053	0.122	0.19
99005	11.969	12.688	13.449	7.828	8.445	9.132	0.14	0.207	0.279

Table 6 Estimated GEV parameters using L-moments technique rainfall data from 1965 to 2018

Station #	Location			Scale			Shape		
	95% lower CI	Estimate	95% upper CI	95% lower CI	Estimate	95% upper CI	95% lower CI	Estimate	95% upper CI
91011	16.318	17.254	18.141	9.855	10.536	11.258	0.007	0.066	0.124
91022	11.682	12.334	13.032	7.259	7.789	8.352	0.02	0.083	0.138
91072	13.331	14.048	14.865	7.73	8.359	8.935	− 0.021	0.047	0.104
91126	13.813	14.628	15.511	8.896	9.525	10.211	0	0.065	0.131
91223	14.088	14.742	15.321	7.127	7.664	8.236	0.068	0.129	0.187
92006	10.021	10.744	11.576	7.996	8.75	9.48	0.246	0.333	0.425
92008	10.231	11.013	11.955	8.6	9.415	10.235	0.238	0.329	0.433
92012	10.271	11.018	11.792	7.654	8.375	9.183	0.213	0.291	0.38
92030	16.131	17.07	18.146	9.835	10.598	11.413	0.092	0.162	0.227
92047	11.05	11.848	12.657	7.912	8.577	9.259	0.192	0.264	0.348
94008	9.103	9.714	10.293	6.462	7.006	7.507	0.132	0.207	0.279
94020	12.666	13.298	13.943	6.613	7.193	7.83	0.161	0.229	0.307
94030	9.533	10.162	10.785	6.504	7.095	7.635	0.168	0.246	0.333
95003	9.731	10.249	10.737	5.828	6.23	6.641	0.003	0.067	0.126
96002	13.598	14.22	14.91	6.91	7.352	7.887	− 0.025	0.038	0.094
97000	16.488	17.092	17.749	7.039	7.565	8.008	− 0.015	0.043	0.097
97047	21.999	22.823	23.659	9.18	9.757	10.417	− 0.106	-0.05	0.005
97054	27.108	28.02	29.021	10.435	11.193	11.972	− 0.037	0.02	0.076
98004	13.67	14.368	15.094	7.493	8.028	8.661	0.05	0.109	0.172
99005	11.91	12.641	13.304	7.741	8.38	9.032	0.123	0.2	0.272

climate indices or elevation above mean sea level (Ragulina and Reitan 2017; Tyralis et al. 2019). However, all the stations located in the high altitude did not produce negative shape parameter due to the non-linear dependency of the shape parameter on elevation. In addition, influence of climate indices on shape parameter was not considered in this research as the analysis was performed considered the rainfall as stationary.

The parameters of the GEV distribution were also estimated for three other time-series: before millennium drought (1965–1996), during millennium drought (1997–2009) and after millennium drought (2010–2018). Due to the space limitation, they were not shown in this paper. Like the whole study period time-series analysis, positive shape parameter was observed for all the selected rainfall stations except two (stations 91072 and 97047) before millennium drought, two stations (stations 97047 and 97054) during millennium drought and two stations (stations 97047 and 91011) after millennium drought. Therefore, the Fréchet (type II) distribution GEV distribution is suitable for modelling monthly maximum of daily rainfall in Tasmania.

All the parameter estimation techniques adopted in this research are showing the same outcomes. Therefore, the GEV parameters estimation technique has negligible impact on the extreme rainfall modelling. Any of the methods can be applied in modelling daily extreme rainfall. However, the length of the data series used for the analysis has some impacts on the parameters values as evidenced from Tables 3, 4, 5, 6. Nevertheless, large samples should be adopted to identify the true behaviour of extreme rainfall (Papalexiou and Koutsoyiannis 2013). Therefore, the distribution that was identified considering the whole study period (1965–2018) is the appropriate distribution for a particular meteorological station.

The analysis of the study was further extended by estimating the return levels of the monthly maximum of the daily rainfall. The return levels were estimated for 2, 5, 10, 20, 50 and 100 years average recurrence interval (ARI). The estimated return levels are shown in Tables 7, 8, 9, 10 for MLE, GMLE, Bayesian and L-moments parameter estimation techniques for the whole study period, i.e. 1965–2018.

Similar to the estimated parameters, there is not much variation of the return levels of the monthly maximum of the daily rainfall for different ARI events. Using different GEV parameters estimation technique, similar return level was observed for the same ARI events for a particular station. The outcomes of the return levels estimation are evidenced from Tables 7, 8, 9, 10 for the whole study period. The same outcomes were observed for the other time-series data before millennium drought, during millennium drought and after millennium drought. To keep the length of the paper minimum, they are not shown here. Therefore, any of the GEV parameters estimation technique could be used to estimate the future daily extreme rainfall.

Table 7 Estimated return level of the monthly maximum daily rainfall (in mm) for difference ARI using the MLE parameter estimation technique

Station #	2 years	5 years	10 years	20 years	50 years	100 years
91011	16.647	26.37	33.594	41.176	52.041	61.036
91022	15.241	24.821	31.665	38.632	48.276	55.994
91072	17.284	27.235	33.978	40.565	49.266	55.919
91126	18.042	29.53	37.742	46.106	57.689	66.964
91223	17.633	27.44	34.748	42.437	53.484	62.654
92006	13.452	27.497	41.74	60.885	97.212	136.665
92008	13.843	28.935	44.365	65.241	105.148	148.799
92012	14.037	26.764	38.305	52.492	76.799	100.739
92030	20.974	34.983	45.922	57.865	75.754	91.222
92047	14.616	27.402	39.26	54.097	80.043	106.101
94008	12.044	21.852	30.301	40.272	56.581	71.941
94020	16.2	26.397	34.582	43.714	57.731	70.143
94030	12.747	23.001	31.8	42.152	59.024	74.861
95003	12.446	19.946	25.359	30.915	38.674	44.94
96002	16.906	25.541	31.495	37.391	45.3	51.44
97000	19.931	28.884	35.013	41.047	49.089	55.291
97047	26.243	37.024	43.979	50.519	58.794	64.858
97054	32.238	45.268	53.975	62.388	73.366	81.658
98004	17.314	27.394	34.852	42.656	53.798	62.991
99005	15.813	27.343	36.593	46.911	62.742	76.755

Table 8 Estimated return level of the monthly maximum of daily rainfall for difference ARI using the GMLE parameter estimation technique

Station #	2 years	5 years	10 years	20 years	50 years	100 years
91011	16.575	26.487	34.008	42.035	53.754	63.636
91022	15.137	24.949	32.154	39.648	50.274	58.984
91072	17.096	27.424	34.735	42.123	52.266	60.318
91126	17.891	29.681	38.379	47.459	60.389	71.031
91223	17.561	27.553	35.154	43.283	55.178	65.232
92006	13.464	27.422	41.501	60.342	95.912	134.359
92008	13.857	28.844	44.072	64.573	103.541	145.934
92012	14.029	26.799	38.414	52.727	77.321	101.609
92030	20.898	35.117	46.405	58.889	77.863	94.506
92047	14.612	27.42	39.317	54.224	80.33	106.587
94008	12.022	21.905	30.489	40.683	57.479	73.411
94020	16.169	26.485	34.86	44.289	58.913	71.991
94030	12.728	23.059	31.991	42.562	59.91	76.301
95003	12.344	20.041	25.78	31.823	40.508	47.723
96002	16.752	25.679	32.092	38.648	47.765	55.096
97000	19.767	29.038	35.654	42.385	51.692	59.135
97047	26.366	36.919	43.581	49.739	57.385	62.884
97054	31.956	45.539	55.067	64.63	77.654	87.915
98004	17.225	27.513	35.307	43.617	55.733	65.937
99005	15.769	27.441	36.927	47.614	64.202	79.051

The visual comparison of the return levels estimation on the adopted parameters estimation techniques are also provided in this research. The plotted results of the return levels are shown from Figs. 2, 3, 4, 5 for the whole study period, before millennium drought, during millennium drought and after millennium drought respectively. The outcomes of four selected rainfall stations (stations 91011, 92012, 96002 and 99005) for different parameter estimation techniques (MLE, GMLE, Bayesian and L-moments) are shown in this paper. All of the figures clearly indicated that the influence of

Table 9 Estimated return level of the monthly maximum of daily rainfall for difference ARI using the Bayesian parameter estimation technique

Station #	2 years	5 years	10 years	20 years	50 years	100 years
91011	16.639	26.418	33.699	41.358	52.355	61.479
91022	15.289	24.943	31.855	38.902	48.674	56.509
91072	17.235	27.233	34.031	40.688	49.509	56.274
91126	18.076	29.637	37.916	46.362	58.077	67.474
91223	17.747	27.639	35.015	42.779	53.938	63.207
92006	13.453	27.587	41.96	61.321	98.149	138.241
92008	13.964	29.205	44.77	65.807	105.98	149.877
92012	14.119	26.955	38.6	52.919	77.46	101.639
92030	20.962	35.06	46.095	58.165	76.283	91.981
92047	14.82	27.772	39.742	54.677	80.71	106.777
94008	12.045	21.91	30.429	40.501	57.012	72.594
94020	16.204	26.454	34.696	43.905	58.063	70.62
94030	12.782	23.088	31.934	42.341	59.308	75.236
95003	12.425	19.975	25.447	31.08	38.975	45.373
96002	16.957	25.667	31.685	37.653	45.673	51.909
97000	19.888	28.885	35.064	41.164	49.319	55.628
97047	26.419	37.28	44.291	50.884	59.231	65.35
97054	32.343	45.45	54.214	62.688	73.752	82.114
98004	17.31	27.438	34.953	42.833	54.11	63.437
99005	15.947	27.591	36.929	47.342	63.315	77.45

Table 10 Estimated return level of the monthly maximum of daily rainfall for difference ARI using the L-moments parameter estimation technique

Station #	2 years	5 years	10 years	20 years	50 years	100 years
91011	16.575	26.301	33.602	41.33	52.504	61.841
91022	15.233	24.774	31.601	38.561	48.208	55.941
91072	17.138	27.035	33.883	40.682	49.828	56.948
91126	18.161	29.636	37.713	45.842	56.945	65.719
91223	17.619	27.424	34.749	42.474	53.597	62.853
92006	14.155	27.765	40.052	55.102	80.786	105.984
92008	14.68	29.264	42.379	58.393	85.624	112.248
92012	14.257	26.771	37.645	50.565	71.863	92.073
92030	21.072	35.06	45.837	57.479	74.708	89.432
92047	15.149	27.631	38.205	50.516	70.353	88.763
94008	12.382	22.037	29.797	38.464	51.782	63.59
94020	16.048	26.177	34.487	43.923	58.696	72.032
94030	12.884	23.03	31.482	41.193	56.604	70.699
95003	12.56	20.076	25.375	30.712	38.013	43.79
96002	16.933	25.566	31.489	37.331	45.133	51.163
97000	19.887	28.81	34.96	41.046	49.207	55.539
97047	26.366	36.919	43.581	49.739	57.385	62.884
97054	32.137	45.059	53.776	62.259	73.42	81.919
98004	17.37	27.45	34.842	42.525	53.408	62.32
99005	15.827	27.301	36.464	46.646	62.204	75.921

parameter estimation techniques on the return levels for different ARI events are minor.

To identify the discrepancy between the observations and the predicted values, goodness of fit test was performed. The example plots of the goodness of fit test for Cape Grim (91011) station is shown in Fig. 6 in terms of probability plot (PP), quantile plot (QQ), density and return level plot. The graphical plot (Fig. 6) of the goodness of fit test suggested that the daily extreme rainfall

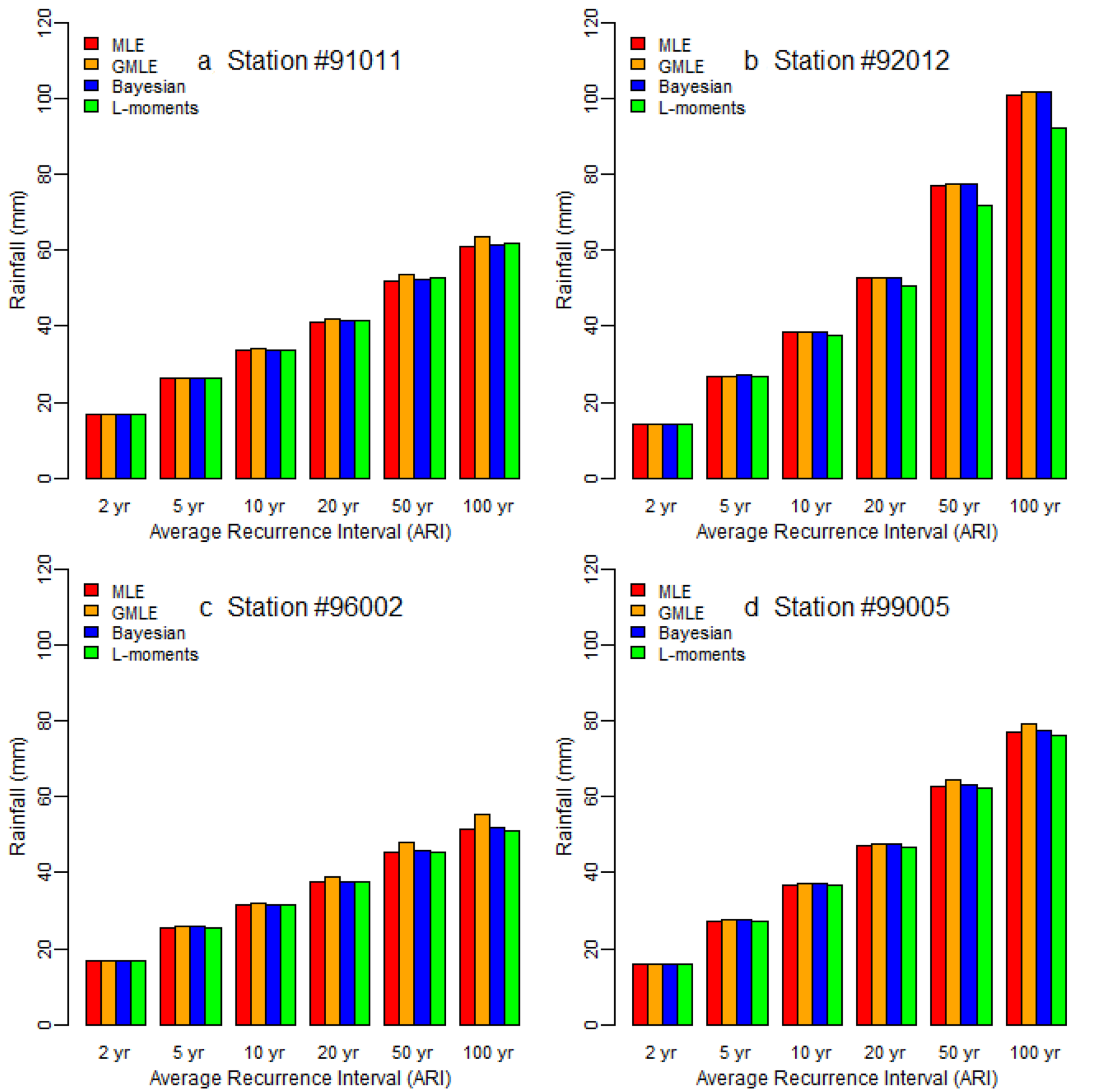

Fig. 2 Comparison of the maximum daily rainfall prediction for different average recurrence interval (ARI) using different GEV parameters estimation techniques for the whole study period (1965–2018)

data set were successfully fitted with the stationary GEV models.

The evaluation of the parameters estimation techniques of the GEV distribution were performed based on Mean Square Error (MSE) and Mean Absolute Error (MAE). The outputs of the error analysis are shown in Table 11. The results of the MSE analysis suggest that GMLE technique has is less error for most of the meteorological stations in the quantile estimation. However, the MAE analysis produced less error for the L-moment parameters estimation method. Nevertheless, there are four rainfall stations (stations #92006, #92008, #92012, #92047) with very high MSE. The presence of higher MSE for these rainfall stations may be due to the

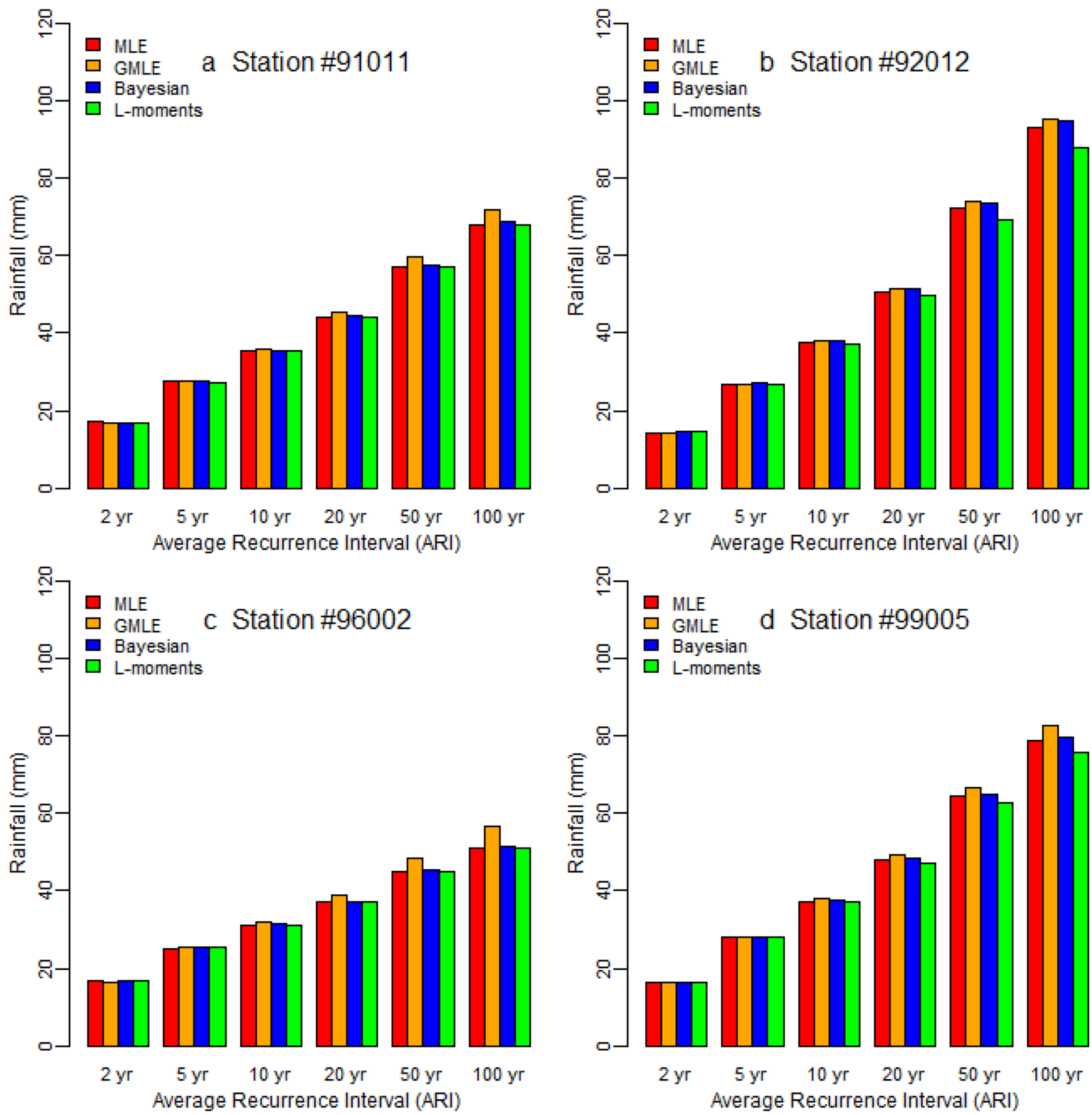

Fig. 3 Comparison of the maximum daily rainfall prediction for different average recurrence interval (ARI) using different GEV parameters estimation techniques before millennium drought (1965–1996)

presence of outliers. It should be noted that outliers were not removed from the original data sets. Although MLE, GMLE and Bayesian methods produced very large MSE for these stations, the L-moments have the least MSE. The MAE of these stations are reasonable as evidence in Table 11. Therefore, we recommend the L-moments method to be adopted for the estimation of parameters for the GEV distribution.

Conclusions and recommendations

In this study, monthly maximum of daily rainfall from 1965 to 2018 were used to estimate the parameters of the generalised extreme value (GEV) distribution using several parameters estimation techniques. Four different GEV parameters estimation techniques used in this study was MLE, GMLE, Bayesian and L-moments. The study was conducted to

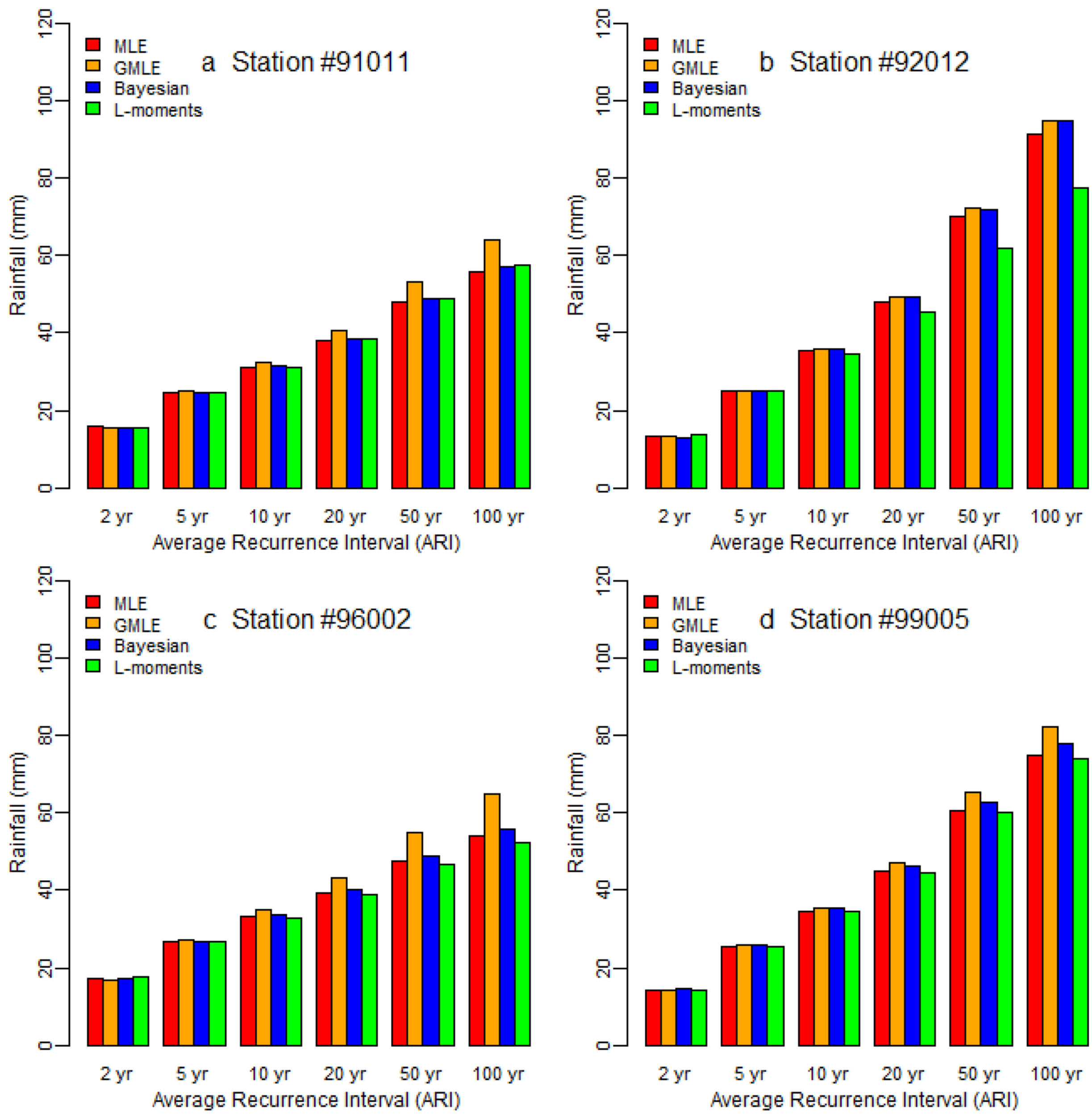

Fig. 4 Comparison of the maximum daily rainfall prediction for different average recurrence interval (ARI) using different GEV parameters estimation techniques during millennium drought (1997–2009)

recommend appropriate parameters selection method for the application of the GEV technique in modelling extreme rainfall. Since the three parameters GEV distribution has been widely applied for describing the extreme climatic events, the method was adopted in this research. The available parameters estimation methods of the GEV distribution were applied on Tasmanian extreme rainfall. The parameters were estimated for four different time-scale data: the whole study period (1965–2018), before millennium drought (1965–1996), during millennium drought (1997–2009) and after millennium drought (2010–2018).

The outcomes of the errors (MSE and MAE) analysis in quantile estimation suggests that L-moments is the best method in estimating the parameters of the GEV

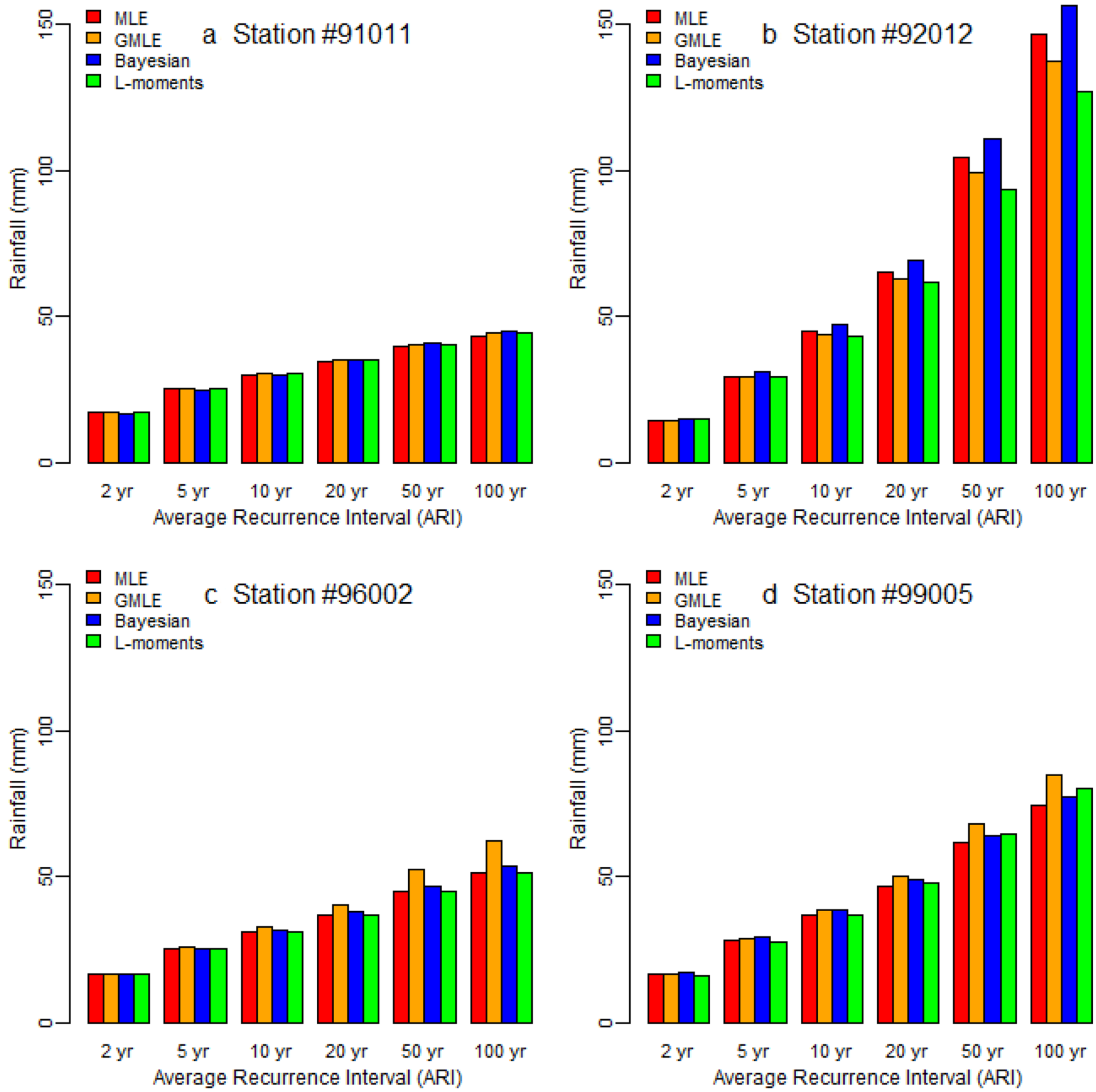

Fig. 5 Comparison of the maximum daily rainfall prediction for different average recurrence interval (ARI) using different GEV parameters estimation techniques after millennium drought (2010–2018)

distribution, especially when there is presence of outliers in the data series. Therefore, the L-moments method should be adopted for the estimation of the GEV parameters for rainfall analysis in Tasmania. This research provides a primary indication for the selection of appropriate GEV parameters estimation techniques in extreme rainfall modelling in Tasmania. Nevertheless, further researches in Tasmania and other regions are required for a generic conclusion. Moreover, the length of the data series has considerable implications on the magnitude of the estimated GEV parameters.

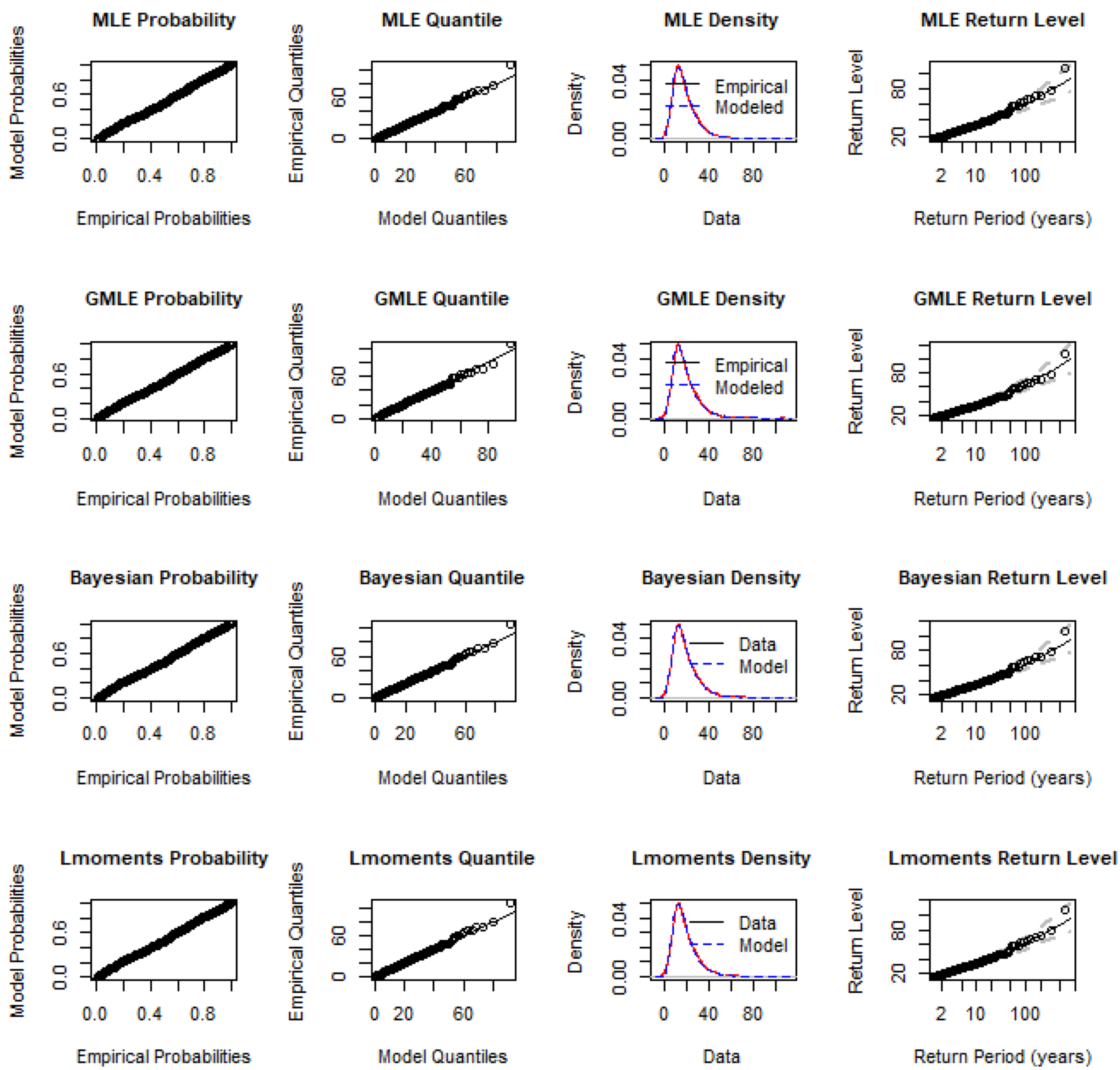

Fig. 6 Probability plot (PP), quantile plot (QQ), density and return level plot for Cape Grim (91011) station

The Fréchet (type II) GEV distribution is suitable for most of the rainfall stations for extreme rainfall modelling.

It should be noted that the spatial analysis of the stations and the GEV distribution parameters were considered in this research. This research can be extended to determine the degree of spatial persistence using the covariance between two random variables (Campling and Gobin 2001). That will allow to determine the potential parameter values of the GEV distribution at unsampled locations. As such, GIS based ordinary kriging which is the weighted moving average interpolation technique using covariance models can be applied.

Table 11 Estimated errors of the GEV models for the selected rainfall stations

Station #	MSE				MAE			
	MLE	GMLE	Bayesian	L-moments	MLE	GMLE	Bayesian	L-moments
91011	0.729	0.467	0.663	0.579	0.340	0.334	0.333	0.331
91022	3.339	2.336	3.142	3.326	0.480	0.582	0.508	0.467
91072	0.949	0.623	0.906	0.677	0.444	0.562	0.462	0.388
91126	1.041	0.922	0.968	1.377	0.478	0.601	0.475	0.464
91223	1.405	0.825	1.238	1.332	0.465	0.481	0.475	0.464
92006	100.304	90.362	100.693	13.176	1.735	1.689	1.737	1.331
92008	140.607	125.822	154.133	17.058	2.157	2.111	2.197	1.587
92012	17.624	18.919	18.694	7.912	0.880	0.880	0.882	0.889
92030	0.587	0.927	0.619	0.764	0.375	0.396	0.376	0.381
92047	55.723	57.143	58.877	17.863	1.443	1.448	1.405	1.331
94008	13.019	15.031	13.661	4.634	0.769	0.785	0.772	0.711
94020	1.708	1.611	1.629	1.794	0.688	0.661	0.687	0.653
94030	3.289	4.123	3.752	1.759	0.483	0.490	0.482	0.501
95003	0.172	0.648	0.186	0.135	0.258	0.336	0.254	0.204
96002	0.454	0.448	0.400	0.504	0.226	0.348	0.228	0.226
97000	0.496	0.364	0.433	0.437	0.344	0.437	0.343	0.334
97047	2.243	2.850	2.207	2.850	0.768	0.697	0.785	0.697
97054	2.262	1.577	2.103	2.060	0.558	0.819	0.587	0.512
98004	0.662	0.622	0.629	0.776	0.358	0.428	0.362	0.359
99005	1.498	1.814	1.547	1.499	0.673	0.668	0.667	0.685

Funding There was no funding for this research.

Availability of data and materials Data are publicly available.

Code availability Not applicable.

Declarations

Conflict of interest There was no conflict of interest.

References

Ávila ÁGFC, Escobar YC, Justino F (2019) Recent precipitation trends and floods in the colombian andes. Water 11:379

Bryson Bates JE, Janice Green, Aurel Griesser, Dörte Jakob, Rex Lau, Eric Lehmann, Michael Leonard, Aloke Phatak, Tony Rafter, Alan Seed, Seth Westra, and Feifei Zheng (2015) Australian Rainfall and Runoff Revision Project 1: Development of Intensity-Frequency-Duration Information Across Australia. Water Engineering: Barton, Australia: Engineers Australia

Buishand TA (1982) Some methods for testing the homogeneity of rainfall records. J Hydrol 58:11–27

Campling P, Gobin A, Feyen JJHp (2001) Temporal and spatial rainfall analysis across a humid tropical catchment. Hydrol Process 15:359–375

Cannon AJ, Innocenti S (2019) Projected intensification of sub-daily and daily rainfall extremes in convection-permitting climate model simulations over North America: implications for future intensity–duration–frequency curves. Nat Hazards Earth Syst Sci 19:421–440

Coles S (2001) An introduction to statistical modeling of extreme values. Springer-Verlag, New York

Coles SG, Dixon MJ (1999) Likelihood-based inference for extreme value models. Extremes 2:5–23

Coles S, Tawn J (2005) Bayesian modelling of extreme surges on the UK east coast. Philos Trans Royal Soc Math Phys Eng Sci 363:1387–1406

Cox PM, Betts RA, Jones CD, Spall SA, Totterdell IJ (2000) Acceleration of global warming due to carbon-cycle feedbacks in a coupled climate model. Nature 408:184–187

Crowley TJ (2000) Causes of climate change over the past 1000 years. Science 289:270

Domonkos P (2015) Homogenization of precipitation time series with ACMANT. Theoret Appl Climatol 122:303–314

DPI (2010) Vulnerability of Tasmania's natural environment to climate change: an overview. depar tment of primar y industries, parks, water and environment, hobart.

El Adlouni S, Ouarda TBMJ, Zhang X, Roy R, Bobée B (2007) Generalized maximum likelihood estimators for the nonstationary generalized extreme value model. Water Resour Res 43(3)

Fischer EM, Knutti R (2015) Anthropogenic contribution to global occurrence of heavy-precipitation and high-temperature extremes. Nat Clim Chang 5:560–564

Ghorbani MA, Kahya E, Roshni T, Kashani MH, Malik A, Heddam S (2021) Entropy analysis and pattern recognition in rainfall data, north Algeria. Theoret Appl Climatol 144:317–326

Gilks WR, Richardson S, Spiegelhalter D (1995) Markov chain monte carlo in practice. Chapman and Hall/CRC, Boca Raton

Hill KJ, Santoso A, England MH (2009) Interannual Tasmanian rainfall variability associated with large-scale climate modes. J Clim 22:4383–4397

Hosking JRM (1990) L-moments: analysis and estimation of distributions using linear combinations of order statistics. J Roy Stat Soc Ser B (methodol) 52:105–124

Hosking JRM, Wallis JR (1993) Some statistics useful in regional frequency analysis. Water Resour Res 29:271–281
Hossain I, Esha R, Alam Imteaz M (2018a) An attempt to use non-linear regression modelling technique in long-term seasonal rainfall forecasting for australian capital territory. Geosciences 8:282
Hossain I, Rasel HM, Imteaz MA, Mekanik F (2018b) Long-term seasonal rainfall forecasting: efficiency of linear modelling technique. Environ Earth Sci 77:280
Hossain I, Rasel HM, Imteaz MA, Mekanik F (2020a) Long-term seasonal rainfall forecasting using linear and non-linear modelling approaches: a case study for Western Australia. Meteorol Atmos Phys 132:331–341
Hossain I, Rasel HM, Mekanik F, Imteaz MA (2020b) Artificial neural network modelling technique in predicting Western Australian seasonal rainfall. Int J Water 14:14–28
Hossain I, Imteaz MA, Khastagir A (2021b) Water footprint: applying the water footprint assessment method to Australian agriculture. J Sci Food Agric 101:4090–4098
Hossain I, Imteaz MA, Khastagir A (2021a) Effects of estimation techniques on generalised extreme value distribution (GEVD) parameters and their spatio-temporal variations. Stoch Environ Res Risk Assess 1–10. https://doi.org/10.1007/s00477-021-02024-x
Huard D, Mailhot A, Duchesne S (2010) Bayesian estimation of intensity–duration–frequency curves and of the return period associated to a given rainfall event. Stoch Env Res Risk Assess 24:337–347
IPCC (2012) Managing the risks of extreme events and disasters to advance climate change adaptation. A special report of working Groups I and II of the intergovernmental panel on climate change.
Katz RW (2013) Statistical methods for nonstationary extremes. In: Aghakouchak A, Easterling D, Hsu K, Schubert S, Sorooshian S (eds) Extremes in a changing climate: detection, analysis and uncertainty. Springer, Netherlands, Dordrecht
Khaliq MN, Ouarda TBMJ (2007) On the critical values of the standard normal homogeneity test (SNHT). Int J Climatol 27:681–687
Khastagir A (2018) Fire frequency analysis for different climatic stations in Victoria, Australia. Nat Hazards 93:787–802
Khastagir A, Jayasuriya N (2010) Optimal sizing of rain water tanks for domestic water conservation. J Hydrol 381:181–188
Khastagir A, Hossain I, Aktar N (2021) Evaluation of different parameter estimation techniques in extreme bushfire modelling for Victoria, Australia. Urban Climate 37:100862
Kumar S, Roshni T, Kahya E, Ghorbani MA (2020) Climate change projections of rainfall and its impact on the cropland suitability for rice and wheat crops in the Sone river command, Bihar. Theoret Appl Climatol 142:433–451
Lai Y, Dzombak DA (2019) Use of historical data to assess regional climate change. J Clim 32:4299–4320
Lazoglou G, Anagnostopoulou C, Tolika K, Kolyva-Machera F (2019) A review of statistical methods to analyze extreme precipitation and temperature events in the Mediterranean region. Theoret Appl Climatol 136:99–117
Loubere P. 2012. The Global Climate System [Online]. Nature Education Knowledge. Available: https://www.nature.com/scitable/knowledge/library/the-global-climate-system-74649049/. Accessed 25 July 2021
Martins ES, Stedinger JR (2000) Generalized maximum-likelihood generalized extreme-value quantile estimators for hydrologic data. Water Resour Res 36:737–744
McMahon TA, Srikanthan R (1981) Log Pearson III distribution—Is it applicable to flood frequency analysis of Australian streams? J Hydrol 52:139–147
Mekanik F, Imteaz MA, Gato-Trinidad S, Elmahdi A (2013) Multiple regression and artificial neural network for long-term rainfall forecasting using large scale climate modes. J Hydrol 503:11–21
Min S-K, Zhang X, Zwiers FW, Hegerl GC (2011) Human contribution to more-intense precipitation extremes. Nature 470:378–381
Nakajima J, Kunihama T, Omori Y, Frühwirth-Schnatter S (2012) Generalized extreme value distribution with time-dependence using the AR and MA models in state space form. Comput Stat Data Anal 56:3241–3259
Papalexiou SM, Koutsoyiannis D (2013) Battle of extreme value distributions: a global survey on extreme daily rainfall. Water Resour Res 49:187–201
Park J-S (2005) A simulation-based hyperparameter selection for quantile estimation of the generalized extreme value distribution. Math Comput Simul 70:227–234
Park J-S, Kang H-S, Lee YS, Kim M-K (2011) Changes in the extreme daily rainfall in South Korea. Int J Climatol 31:2290–2299
Pereira VR, Blain GC, Avila AMHd, Pires RCdM, Pinto HS (2018) Impacts of climate change on drought: changes to drier conditions at the beginning of the crop growing season in southern Brazil. J Bragantia 77:201–211
Pfahl S, O'Gorman PA, Fischer EM (2017) Understanding the regional pattern of projected future changes in extreme precipitation. Nat Clim Chang 7:423
Ragulina G, Reitan T (2017) Generalized extreme value shape parameter and its nature for extreme precipitation using long time series and the Bayesian approach. Hydrol Sci J 62:863–879
Sachindra DA, Ng AWM, Muthukumaran S, Perera BJC (2016) Impact of climate change on urban heat island effect and extreme temperatures: a case-study. Q J R Meteorol Soc 142:172–186
Sillmann J, Thorarinsdottir T, Keenlyside N, Schaller N, Alexander LV, Hegerl G, Seneviratne SI, Vautard R, Zhang X, Zwiers FW (2017) Understanding, modeling and predicting weather and climate extremes: challenges and opportunities. Weather Clim Extremes 18:65–74
Towler E, Rajagopalan B, Gilleland E, Summers RS, Yates D, Katz RW (2010) Modeling hydrologic and water quality extremes in a changing climate: a statistical approach based on extreme value theory. Water Resour Res 46(11)
Tyralis H, Papacharalampous G, Tantanee S (2019) How to explain and predict the shape parameter of the generalized extreme value distribution of streamflow extremes using a big dataset. J Hydrol 574:628–645
Westra S, Alexander LV, Zwiers FW (2012) Global increasing trends in annual maximum daily precipitation. J Clim 26:3904–3918
Wijngaard JB, Klein Tank AMG, Können GP (2003) Homogeneity of 20th century european daily temperature and precipitation series. Int J Climatol 23:679–692
Xavier ACF, Blain GC, Morais MVBd, Sobierajski GdR (2019) Selecting the best nonstationary generalized extreme value (GEV) distribution: on the influence of different numbers of GEV-models. J Bragantia 78:606–621
Yilmaz AG, Perera BJC (2014) Extreme rainfall nonstationarity investigation and intensity–frequency–duration relationship. J Hydrol Eng 19:1160–1172
Yilmaz AG, Hossain I, Perera BJC (2014) Effect of climate change and variability on extreme rainfall intensity–frequency–duration relationships: a case study of Melbourne. Hydrol Earth Syst Sci 18:4065–4076
Yoon S, Cho W, Heo J-H, Kim CE (2010) A full Bayesian approach to generalized maximum likelihood estimation of generalized extreme value distribution. Stoch Env Res Risk Assess 24:761–770

Publisher's Note Springer Nature remains neutral with regard to jurisdictional claims in published maps and institutional affiliations.